Optimal Pick-up Locations for Transport and Handling of Limp Materials

Part I: One-Dimensional Strips

SHRINIVAS LANKALAPALLI[1]

Scientific Computation Research Center, Rensselaer Polytechnic Institute, Troy, New York 12180, U.S.A.

JEFFREY W. EISCHEN[2]

Department of Mechanical & Aerospace Engineering, North Carolina State University, Raleigh, North Carolina 27695, U.S.A.

ABSTRACT

Pick-up locations are obtained on strips of limp material that minimize a measure of deformation (strain energy). The strips are modeled as continuous beams subjected to a uniformly distributed load using small and large deflection beam theories. Pick-up locations correspond to n support locations of the continuous beam. Strain energy is computed from a finite element solution, and optimal locations are obtained by solving unconstrained and bound constrained optimization problems. Results are in terms of a nondimensional number that characterizes the flexibility of the beam and are applicable to a wide range of limp materials. Some results for fabric strips are also presented.

Limp materials are used in many economically important industries such as textiles, aerospace, automobiles, and leather. Most of the tasks involving the handling of limp materials are done manually, which make them labor intensive and time consuming. Automatic handling systems that can be reprogrammed to perform a different task in relation to rigid objects are readily available. These are often robot systems, and the reprogramming involves defining a new set of end-effector trajectories than can be repeated. Application of similar systems for handling limp materials will reduce the time associated with manual handling, lower costs, and increase quality, thus increasing productivity. This, however, is a challenging task, primarily because the low bending stiffness of limp materials makes them easily susceptible to large deformations and rotations. As a result, limp parts can easily change shape during handling. In addition, there are huge variations in the bending, friction, and tensile properties of different limp materials, which are further influenced by environmental conditions. These unique properties and behavior of limp materials present numerous problems when using sensory robotics to automate their handling.

Most manufacturing operations are performed on limp material parts that are initially flat. The pick and place operation is a basic one for handling and transporting limp parts during various manufacturing processes. This operation can be automated using robots equipped with suitable end effectors and sensors. For ease of manipulation by robots, it is essential that limp parts do not change shape during handling. This can be ensured by picking up the limp parts such that they undergo minimum deformation. In general, limp parts come in various shapes, and the amount of deformation they undergo is a function of pick-up locations. In this research, we develop procedures to solve for optimal pick-up locations that result in minimum deformation of limp parts of different shapes (see Figure 1). We model the limp parts as beams and shells undergoing large deformations and rotations using geometrically exact nonlinear finite element formulations, and find the optimal locations by solving an optimization problem in which a measure of the deformation as a function of pick-up locations is minimized. We anticipate that *a priori* knowledge of pick-up locations for parts of different shapes will reduce sensory requirements and facilitate offline programming of robots for limp material handling.

In this paper, we restrict ourselves to the problem of optimal pick-up locations for one-dimensional strips, which are modeled as flexible beams. In a subsequent

[1] Corresponding author, post doctoral research associate, tel: 518-276-6195, fax: 518-276-4886, email: slankal@scorec.rpi.edu

[2] Associate professor, email: eischen@eos.ncsu.edu

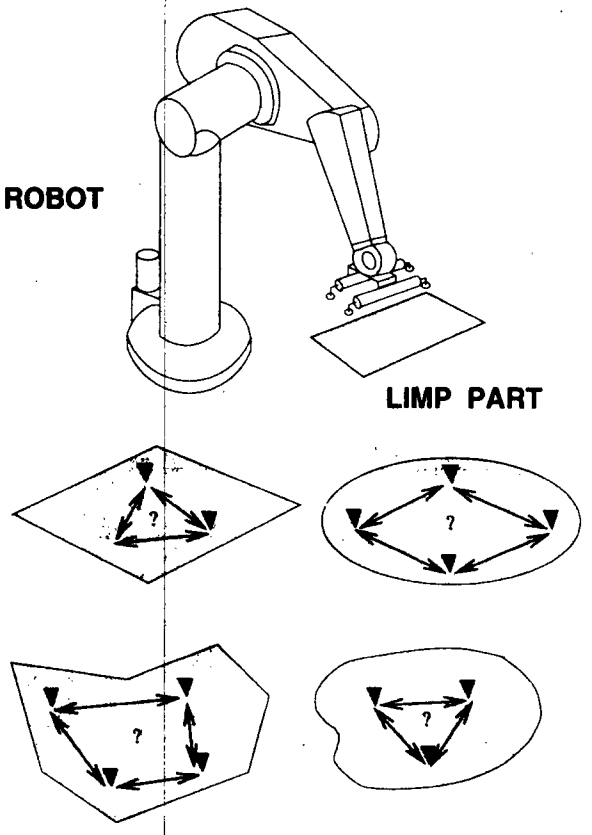

FIGURE 1. Pick-up locations for limp parts.

paper comprising Part II of this work, we solve the problem for two-dimensional limp parts.

Literature Review

In literature, several works focus on the problem of automating the handling of limp materials. Early research for textile applications focussed on the development of retrieval devices for destacking operations in apparel manufacturing where a single ply of fabric is to be separated from a stack. Various robotic end-effectors to grip fabric parts were developed, including a gripper based on the pin and adhesive concept by Parker *et al.* [14], an electrostatic gripper by Taylor *et al.* [23], and a flat-surface gripper based on the operational principle of suction and pressure differential by Kolluru *et al.* [10]. Karakerezis *et al.* [8] provided a literature survey of various gripping mechanisms and principles used for gripping flat non-rigid materials.

Vision-guided robotic fabric manipulation was developed and implemented by Torgerson *et al.* [24]. They generated robot motion paths from visual information of fabric edges and demonstrated manipulation of polygonal and nonpolygonal fabric parts. More recently, some automated robotic handling systems have emerged. Czarnecki [3] developed a robotic handling cell for garment manufacture in which garment piece parts are separated from a multi-ply stack and loaded onto a hanger. Fahantidis *et al.* [7] developed a robotic system incorporating vision and force/torque sensing for handling flat textile materials. They presented experimental results for the tasks of grasping, folding, laying, and sweeping of fabric parts.

Modeling and simulation of limp material handling operations is of great use in optimizing the design of manufacturing lines to adapt to limp materials with different physical properties and shapes. In addition, simulation results can facilitate offline programming of robots, thus leading to flexible automation. Eischen *et al.* [5] optimized fabric manipulation during pick and place operations using large displacement beam theory and finite elements to simulate fabric drape, manipulation, and contact. They also developed software based on nonlinear shell theory to simulate 3D motions related to real fabric manufacturing processes [6] and presented numerical simulations of fabric draping and folding. Cugini *et al.* [1, 2] developed a software environment to model and simulate non-rigid material behavior during handling operations.

In mechanics literature, there are some works on the optimal support locations for beams, columns, and plates. Mroz *et al.* [11] derived support locations for minimum compliance of elastic beams, maximum safety factors of plastic collapse for plastic beams, and optimal design with varying cross sections and support positions. Prager *et al.* [16] established criteria for optimal location of supports and steps in the yield moment for plastic design of beams. Rozvany *et al.* [18] derived conditions for the optimal location of segment boundaries and internal supports for column design. Olhoff *et al.* [13] designed continuous columns for minimum total costs of material and interior supports. All these works used classical optimization tools for finding the maxima and minima of functions and functionals.

More recently, Narita [12] used a gradient technique to find support locations that maximize the fundamental natural frequency of beam and plate structures. Wang *et al.* [25] used genetic algorithms to find optimal rigid and elastic support locations for beams with different boundary conditions. Xiang *et al.* [27] used the simplex method of Nelder and Mead to solve for optimal locations of point supports to maximize the fundamental frequency of vibrating plates of different shapes. Wang *et al.* [26] used the same optimization method to find optimal support points that maximize the fundamental frequency of laminated rectangular plates. In all these vibration problems, the objective function was computed using the Rayleigh-

Ritz method. Pitarresi *et al.* [15] presented a simple technique that uses a two-dimensional nonlinear least-squares fit of natural frequency versus support location data for rapid estimation of optimal support locations for vibrating plates. Roschke [17] used an iterative method based on Powell's conjugate directions to find optimal pick-up locations that minimize the absolute value of principle stresses in beams and plates. Objective functions were computed from a finite element solution.

The problem of finding optimal locations for beams, plates, shells, and other structures that minimize strain energy has not, to the best of our knowledge, been solved in the literature. This may perhaps be due to the lack of real applications and the difficulty of obtaining analytical solutions. In this work, we solve for optimal pick-up locations that minimize the strain energy of limp parts. We choose to minimize the strain energy because it is a measure of the average curvature of the limp part and in some sense the average deflection. We model the limp parts as beams and shells undergoing large deformations and rotations by geometrically exact finite element formulations. We then compute the strain energy from the finite element solution for deformation, which requires discretization of the domain of the limp part by a mesh. We also develop procedures that use unconstrained and bound constrained optimization techniques to solve for optimal locations.

Modeling Limp Parts

Strips of limp materials can be considered one-dimensional and are modeled as flexible beams. We first used small deflection beam theory to model the strips because some analytical work for optimal locations was possible with this model. However, as the number of locations increased, the analytical procedure became cumbersome, and we resorted to a numerical solution using a finite element model with standard Euler-Bernoulli beam elements. Next, we gradually lowered the flexibility of the strip, thus allowing for large deflections. In this case, we used a finite element formulation based on large deflection beam theory to model the strip. This formulation is derived from the geometrically exact nonlinear shell finite element formulation used to model two-dimensional limp parts in Part II of this work. Large deflection beam theory is recovered from nonlinear shell theory by setting the Poisson's ratio $\nu = 0$ in the formulation. This can be seen by considering the flexural rigidity D of shells given by

$$D = \frac{Et^3}{12(1 - \nu^2)}$$

where E is Young's modulus and t is the shell thickness. When $\nu = 0$, D reduces to EI, the flexural rigidity per unit width for beams.

Next we provide a brief overview of the nonlinear shell finite element formulation and refer the reader to Deng [4] for complete details.

Shell Finite Element Formulation

The finite element formulation is based on the geometrically exact shell theory conceived by Simo *et al.* [20, 21, 22]. Limp parts are modeled as flexible, doubly curved shells that can accommodate stretching, bending, and transverse shear deformations. Shell theory based on large deformations and rotations is used to formulate a finite element solution strategy.

The kinematic description of the shell starts by parameterizing the position of points within the shell, both on and off the midsurface. Referring to Figure 2, points off the midsurface are located by a position vector $\mathbf{\Phi}$,

$$\mathbf{\Phi}(\xi^1, \xi^2, \xi) = \boldsymbol{\phi}(\xi^1, \xi^2) + \xi \mathbf{t}(\xi^1, \xi^2) \quad , \qquad (1)$$

where $\boldsymbol{\phi}$ is a position vector locating points on the midsurface (reference surface) of the shell. The vector $\mathbf{t}$ is called the director and is a unit vector directed along fibers in the shell that are initially perpendicular to the reference surface. The coordinate ξ measures the distances between the mid-surface and points off the mid-surface along $\mathbf{t}$. The coordinates ξ^1 and ξ^2 serve to parameterize the midsurface and are not necessarily cur-

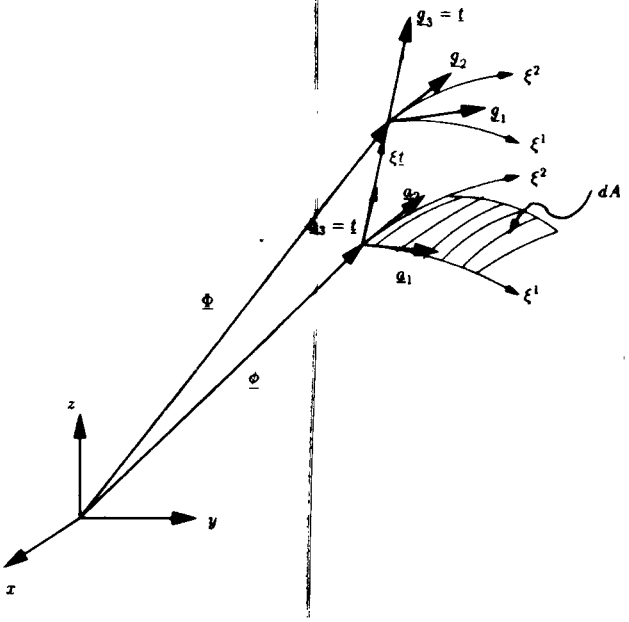

FIGURE 2. Configuration of the shell: $\mathbf{a}_\alpha = \boldsymbol{\phi}_{,\alpha}$ and $\mathbf{g}_\alpha = \mathbf{a}_\alpha + \xi \mathbf{t}_{,\alpha}$ ($\alpha = 1, 2$) are the tangent base vectors at points on and off the midsurface of the shell, respectively.

vilinear surface coordinates. In fact, for this formulation, we have selected these coordinates to be the "parent element coordinates" for the standard isoparametric quadrilateral element. Note that the unit vector $\mathbf{t}$ is not necessarily normal to the midsurface of the deformed shell, thus admitting the possibility of transverse shear strain. The through-thickness coordinate ξ is in the range $-t/2 \leq \xi \leq t/2$, where t is the shell thickness. The undeformed configuration of the shell is given by

$$\boldsymbol{\Phi}_0(\xi^1, \xi^2, \xi) = \boldsymbol{\phi}_0(\xi^1, \xi^2) + \xi \mathbf{t}_0(\xi^1, \xi^2) \quad , \qquad (2)$$

where $\boldsymbol{\phi}_0$ is a vector locating points on the undeformed midsurface, and $\mathbf{t}_0$ is the director in the initial configuration, assumed normal to the midsurface. The essential problem is to determine the evolution of $\boldsymbol{\phi}$ and $\mathbf{t}$ as the shell deforms under its own weight or is manipulated in some way.

The evolution of the unit director vectors $\mathbf{t}(\xi^1, \xi^2)$ during motion of the shell depends on an orthogonal transformation matrix $\boldsymbol{\Lambda}$. Let $\mathbf{t} = \boldsymbol{\Lambda}\mathbf{E}$, where $\boldsymbol{\Lambda}$ is an orthogonal matrix such that $\boldsymbol{\Lambda}\boldsymbol{\Lambda}^T = \mathbf{I}$, and $\mathbf{E}$ is an inertially fixed unit vector. Thus, to determine $\mathbf{t}$ during shell motion, it is sufficient (or equivalent) to determine the matrix $\boldsymbol{\Lambda}$. At any point on the shell, this matrix is related to the unit director vector according to

$$\boldsymbol{\Lambda} = (\mathbf{E}\cdot\mathbf{t})(\mathbf{I} + \widehat{\mathbf{E}\times\mathbf{t}} + \frac{1}{1+\mathbf{E}\cdot\mathbf{t}}(\mathbf{E}\times\mathbf{t}) \otimes (\mathbf{E}\times\mathbf{t}) \quad , \qquad (3)$$

where $\widehat{\ }$ indicates the skew symmetric matrix associated with the indicated vector, and $\otimes$ represents a tensor outer product operator.

Enforcing linear and angular momentum allows development of a weak (or variational) form of the nonlinear shell theory. After incorporating the material response, standard finite element linearization procedures lead to a matrix equation of the form

$$\mathbf{K}(\boldsymbol{\phi}, \mathbf{t}) \begin{Bmatrix} \Delta\boldsymbol{\phi} \\ \Delta\mathbf{t} \end{Bmatrix} = \mathbf{F}_{ext} - \mathbf{P}(\boldsymbol{\phi}, \mathbf{t}) \quad , \qquad (4)$$

where $\mathbf{K}(\boldsymbol{\phi}, \mathbf{t})$ is the tangent stiffness matrix, $\mathbf{P}(\boldsymbol{\phi}, \mathbf{t})$ is the internal force vector, $\mathbf{F}_{ext}$ is the external force vector, and $\boldsymbol{\phi}$ and $\mathbf{t}$ are interpolated between nodal values by standard bilinear isoparametric shape functions. An iterative solution of this matrix equation by an adaptive arc-length control algorithm (see Schweizerhof *et al.* [19]) generates an incremental displacement vector $\Delta\boldsymbol{\phi}$ that is used to update the position of the shell midsurface, together with an incremental rotation matrix $\Delta\boldsymbol{\Lambda}$ that is used to update the directors as the shell deforms.

MINIMIZATION PROBLEM FOR ONE-DIMENSIONAL STRIPS

The problem of optimal pick-up locations that minimize the strain energy of a strip is the same as that of optimal support locations that minimize the strain energy of continuous beams with uniformly distributed load. Figure 3 shows a continuous beam of length l supported at n points, x_i are the support locations measured from the left end, and w is the distributed load per unit length. The support locations correspond to the pick-up locations, and the distributed load is the self weight of the strip. The optimization problem for support locations may be stated as

$$\min f(\mathbf{x}) : \mathbb{R}^n \rightarrow \mathbb{R} \quad ,$$

$$x_i \in [0, l] \qquad (5)$$

where $\mathbf{x}$ is a $(n \times 1)$ vector of support locations and f is the strain energy objective function.

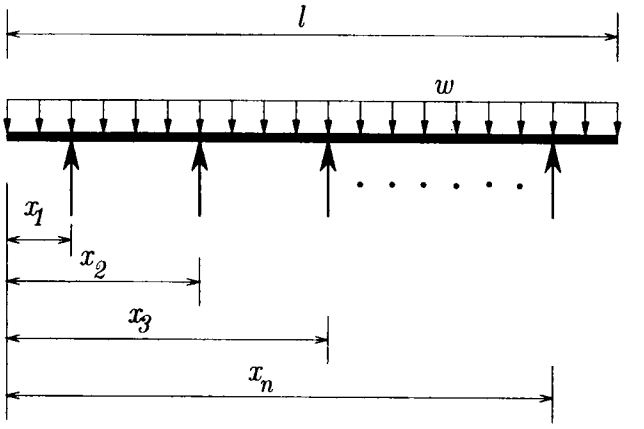

FIGURE 3. Beam supported at n positions.

Beams Undergoing Small Deformations

We first solved the problem for beams undergoing small deformations, as an analytical expression for strain energy is available. This allowed us to quickly check our optimization algorithms. The strain energy U_m for beams undergoing small deformations is given by the well known formula,

$$U_m = \int_0^l \frac{M^2(x)}{2EI}\, dx \quad , \qquad (6)$$

where $M(x)$ is the bending moment, I is the second moment of area, and E is Young's modulus. When $n = 2$, the problem is statically determinate, and we can

write the following expression for strain energy by evaluating Equation 6:

$$U_m = \frac{w^2 l^5}{240EI}\left\{10\left(\frac{x_1}{l}\right)^3\left(\frac{x_2}{l}\right) - 5\left(\frac{x_1}{l}\right)^3 - 5\left(\frac{x_1}{l}\right)^2\left(\frac{x_2}{l}\right) + 10\left(\frac{x_1}{l}\right)^2\left(\frac{x_2}{l}\right)^2 + 40\left(\frac{x_1}{l}\right)\left(\frac{x_2}{l}\right) - 45\left(\frac{x_1}{l}\right)\left(\frac{x_2}{l}\right)^2 - 10\left(\frac{x_1}{l}\right) + 10\left(\frac{x_1}{l}\right)\left(\frac{x_2}{l}\right)^3 + 20\left(\frac{x_2}{l}\right)^2 - 5\left(\frac{x_2}{l}\right)^3 + 6 - 20\left(\frac{x_2}{l}\right)\right\} \quad . \quad (7)$$

The necessary condition for a local minimizer yields two nonlinear simultaneous equations:

$$\frac{\partial U_m}{\partial\left(\frac{x_1}{l}\right)} = 30\left(\frac{x_2}{l}\right)\left(\frac{x_1}{l}\right)^2 - 15\left(\frac{x_1}{l}\right)^2 - 10\left(\frac{x_1}{l}\right)\left(\frac{x_2}{l}\right) + 20\left(\frac{x_1}{l}\right)\left(\frac{x_2}{l}\right)^2 + 40\left(\frac{x_2}{l}\right) - 45\left(\frac{x_2}{l}\right)^2 - 10 + 10\left(\frac{x_2}{l}\right)^3 = 0 \quad , \quad (8)$$

$$\frac{\partial U_m}{\partial\left(\frac{x_2}{l}\right)} = 10\left(\frac{x_1}{l}\right)^3 - 5\left(\frac{x_1}{l}\right)^2 + 20\left(\frac{x_2}{l}\right)\left(\frac{x_1}{l}\right)^2 + 40\left(\frac{x_1}{l}\right) - 90\left(\frac{x_1}{l}\right)\left(\frac{x_2}{l}\right) + 30\left(\frac{x_1}{l}\right)\left(\frac{x_2}{l}\right)^2 + 40\left(\frac{x_2}{l}\right) - 15\left(\frac{x_2}{l}\right)^2 - 20 = 0 \quad . \quad (9)$$

The roots of Equations 8 and 9 obtained using the *fsolve* function of MAPLE with $\frac{x_1}{l} \in [0, 0.5]$ and $\frac{x_2}{l} \in [0.5, 1.0]$ are

$$\left(\frac{x_1}{l}\right)_m = 0.2247 \quad \left(\frac{x_2}{l}\right)_m = 0.7753 \quad .$$

Figure 4 shows a plot of U_m $\left(\text{with } \frac{w^2 l^5}{240EI} = 1.0\right)$ as a function of the support locations. We can verify from the plot that $\left(\frac{x_1}{l}\right)_m$ and $\left(\frac{x_2}{l}\right)_m$ are indeed the global minimizers.

When $n \geq 3$, the analytical procedure is cumbersome due to static indeterminancy, and it leads to long expressions. However, by discretizing the beam by finite elements, the strain energy can be computed in a straightforward manner. We can solve for the optimal locations by using a minimization algorithm with the objective function computed from a finite element solution.

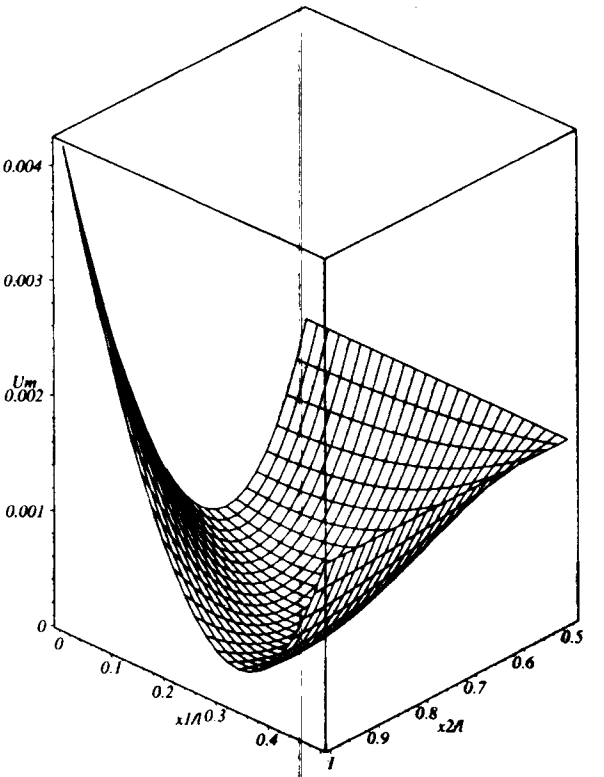

FIGURE 4. Strain energy for two supports.

NUMERICAL SOLUTION PROCEDURE

We use standard Euler-Bernoulli beam elements to discretize the beam and compute the strain energy U_m with the following formula:

$$U_m = \tfrac{1}{2}\,\mathbf{d}^T\mathbf{K}\mathbf{d} \quad . \quad (10)$$

where $\mathbf{K}$ is the stiffness matrix and $\mathbf{d}$ is the vector of nodal displacements and rotations obtained after solving the finite element equations. In order to solve the problem in Equation 5 as a continuous optimization problem, we need to be able to compute the objective function and its gradient for any given support locations. These support locations correspond to enforcing boundary conditions, which can be done only at nodes in the mesh. Hence, whenever the objective function is computed, we automatically generate a mesh with nodes located at support locations. Since the domain is one-dimensional, automatic meshing is easily accomplished by distributing the number of elements in each span based on ratios of span lengths. The gradient is obtained by finite differ-

ences and requires additional objective function computations with perturbed coordinates of the nodes at which the boundary conditions are enforced.

It is possible to solve for optimal locations using an unconstrained optimization method. The bound constraints are never violated during the optimization process. All numerical computations are done in MATLAB. For this purpose, we use a MATLAB function that computes the strain energy of a beam by the finite element method, given a vector of support locations. We employ the Broyden, Fletcher, Goldfarb, and Shanno (BFGS) method for unconstrained minimization to solve for the optimal locations. MATLAB code **bfgswopt** from Kelley [9] implements the algorithm, so we have used it. We compute the gradient by central differences and choose the stopping tolerance for the optimization routine such that the norm of the gradient is reduced by at least five orders of magnitude.

We use a level of discretization of at least ten elements per span of the beam. In some cases, a finer mesh is required to satisfy the stopping criteria. We have chosen as the initial guess the centers of each of the p equal divisions of the beam, where p is the number of supports. For example, when $p = 2$, the initial guess is $[0.25l, 0.75l]$ where l is the length of the beam. Any other initial guess results in a greater number of iterations to converge to the solution.

RESULTS

We have obtained optimal support locations for minimum strain energy up to eight supports. Table I lists numerical values. The solution for the $n = 2$ statically determinate case can be verified to be the same as the one obtained previously by analytical methods. Deflection curves corresponding to 2, 3, 4, and 5 optimal locations are shown in Figure 5a. The optimal locations are symmetrically placed about the centerline, as expected. Spacings between adjacent internal support locations are equal, and as n increases, the outer two support locations move closer to the ends. In general, as the number of support locations increases, the algorithm takes more iterations to achieve the desired reduction in the gradient norm.

TABLE I. Optimal locations for small deformations.

	Number of supports						
Location	2	3	4	5	6	7	8
$\frac{x_1}{l}$	0.2247	0.1450	0.1070	0.0848	0.0702	0.0599	0.0522
$\frac{x_2}{l}$	0.7753	0.5	0.3690	0.2924	0.2421	0.2066	0.1802
$\frac{x_3}{l}$	–	0.8550	0.6310	0.5	0.4140	0.3533	0.3081
$\frac{x_4}{l}$	–	–	0.8930	0.7076	0.5860	0.5	0.4360
$\frac{x_5}{l}$	–	–	–	0.9152	0.7579	0.6467	0.5640
$\frac{x_6}{l}$	–	–	–	–	0.9298	0.7934	0.6919
$\frac{x_7}{l}$	–	–	–	–	–	0.9401	0.8198
$\frac{x_8}{l}$	–	–	–	–	–	–	0.9478

Beams Undergoing Large Deformations

For beams undergoing large deformations, it is not possible to write closed form expressions for strain energy. We solve for optimal locations numerically.

NUMERICAL SOLUTION PROCEDURE

We use the geometrically exact nonlinear shell finite element formulation described earlier to model beams undergoing large deformations. Beam theory is recovered by setting Poisson's ratio $\nu = 0$ in the shell formulation, and the beam is discretized by quadrilateral shell elements. Boundary conditions at the support points restrain both transverse and axial displacements. The strain energy is computed from the finite element solution by summing the areas under load deflection curves of all the nodes in the mesh. This is conveniently done by approximating the area due to each load step by that of a trapezoid as shown in Figure 6. The following formula for strain energy (SE) can be written as

$$SE = \sum_{i=1}^{nodes} \sum^{nsteps} \frac{1}{2}(f_i + f_{i-1})(d_i - d_{i-1}) \quad , \quad (11)$$

where *nsteps* is the total number of load steps, and f_i and d_i are the nodal force and the nodal displacement, respectively, at the end of load step i. Note that the only nodal forces are those due to the self-weight of the beam. Nodal forces developed at hard reaction points do not contribute to strain energy. The load deflection curve needs to be traced accurately to compute the strain energy. We can ensure this by using suitable parameters in the arc-length control algorithm used to solve the nonlinear finite element equations.

A nondimensional parameter $\alpha = \frac{wl^3}{EI}$ characterizes the flexibility of the beam. The greater the value of α, the larger the deformation of the beam. An algorithm for automatic meshing of the beam by quadrilateral elements similar to that used for beams undergoing small deformations, enables us to compute the objective function for

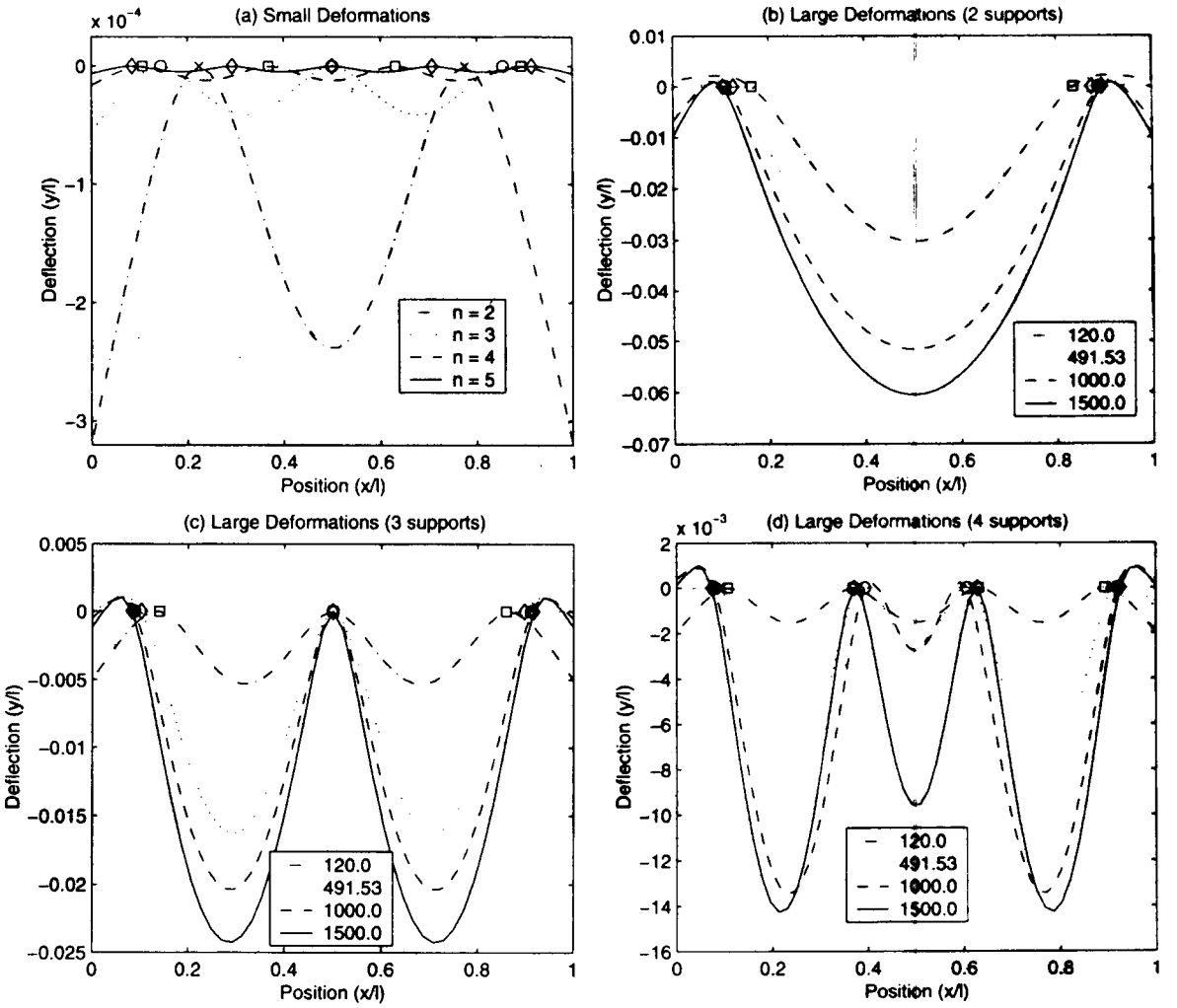

FIGURE 5. Deflection curves of beams undergoing small and large deformations.

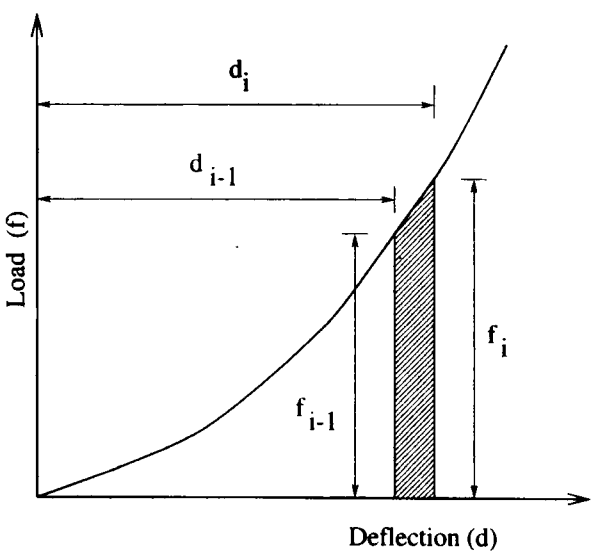

FIGURE 6. Area under a nodal load deflection curve.

any support location. We solve for the optimal locations using the L-BFGS-B code for bound constrained optimization developed by Zhu *et al.* [28], and we use two built-in stopping tests based on the projected gradient and the relative reduction of objective function f to terminate the optimization. The relative reduction of $f = \dfrac{(f_k - f_{k+1})}{\max(|f_{k+1}|, |f_k|, 1)}$, where f_k and f_{k+1} are the objective function values at iterations k and $k + 1$, respectively. If the relative reduction of $f \leq factr*epsmch$, where *epsmch* is the machine precision, or the infinity norm of the projected gradient $\leq pgtol$, the iteration is stopped. We used values of $factr = 1.0$ and $pgtol = 1e^{-8}$ and computed the gradient by finite differences. All variables were bounded between 0 and l (*i.e.*, $0 \leq x_i \leq l$), and the level of discretization is at least ten elements per span of the

beam. We have tried different initial guesses, and all of them result in the same solution.

RESULTS

We obtained optimal support locations for minimum strain energy up to four supports. Tables II, III, and IV show optimal locations for different values of α for $n = 2, 3$, and 4, supports respectively. The locations are symmetrically placed, and as the value of α increases, the end support locations move toward the two ends of the beam. The spacings between adjacent supports need not be equal, as is the case with beams undergoing small deflections. Typical deflection curves for $n = 2, 3$, and 4 supports are shown in Figures 5b, c, and d, respectively. An interesting feature is that the deflection can be up or down along the length of the beam for large deformations, whereas the deflection is always down for small deformations.

TABLE II. Optimal locations for two supports (large deformations).

	α						
Location	7.68	61.44	120.0	491.53	1000.0	1200.0	1500.0
$\frac{x_1}{l}$	0.2246	0.1879	0.1639	0.1255	0.1098	0.1071	0.1038
$\frac{x_2}{l}$	0.7754	0.8121	0.8361	0.8745	0.8902	0.8929	0.8962

TABLE III. Optimal locations for three supports (large deformations).

	α						
Location	7.68	61.44	120.0	491.53	1000.0	1200.0	1500.0
$\frac{x_1}{l}$	0.1451	0.1440	0.1400	0.1022	0.0880	0.0855	0.0827
$\frac{x_2}{l}$	0.5	0.5	0.5	0.5	0.5	0.5	0.5
$\frac{x_3}{l}$	0.8549	0.8560	0.8600	0.8978	0.9120	0.9145	0.9173

TABLE IV. Optimal locations for four supports (large deformations).

	α						
Location	7.68	61.44	120.0	491.53	1000.0	1200.0	1500.0
$\frac{x_1}{l}$	0.1074	0.1068	0.1064	0.0937	0.0800	0.0777	0.0738
$\frac{x_2}{l}$	0.3694	0.3690	0.3688	0.3802	0.3937	0.3929	0.3710
$\frac{x_3}{l}$	0.6306	0.6310	0.6312	0.6198	0.6023	0.6071	0.6290
$\frac{x_4}{l}$	0.8926	0.8932	0.8936	0.9063	0.9100	0.9223	0.9262

Optimal Pick-up Locations for Fabric Strips

In order to demonstrate a practical application of our procedures, we obtained optimal pick-up locations for fabric strips. We measured the material properties of different fabrics with the FAST [29] system—thickness t with the compression meter and the flexural rigidity B in both the warp and weft directions with the bending meter. We computed Young's modulus E as follows:

$$E = \frac{Bb}{I}$$

where $I = \frac{1}{12} bt^3$ with b = width of strip. We measured the weight density w directly. The material properties of four different fabrics are listed in Table V. Figure 7 shows the deformed shapes of different fabric strips when picked at optimal locations, along with strip dimensions and numerical values of optimal locations. We used Young's modulus in the warp direction E_{warp} in all results.

TABLE V. Fabric material properties.

Fabric type	Thickness, mm	Weight/area, gmf/cm²	Youngs modulus, gmf/cm²	
			Warp	Weft
Blue denim	1.142	0.0431	44499.27	15646.2
Cotton twill style 423	0.601	0.0264	75507.65	34091.23
Cotton polyester style 7436	0.402	0.0156	21089.3	19206.36
1000 Denier cordura	0.594	0.0312	83760.48	78623.95

Conclusions

In this paper, we have developed a procedure to solve for optimal pick-up locations that minimize the strain energy of strips of limp materials. We model the strips as beams undergoing large deformations and compute the objective function from a finite element solution. Unconstrained and bound constrained optimization methods are used to solve for optimal locations. Results obtained in terms of nondimensional numbers are applicable to a wide range of limp materials. The effect of flexibility is to cause the outer two locations to move toward the outside and non-uniform intermediate support spacings.

ACKNOWLEDGMENTS

This research was funded by the National Textile Center, and we gratefully acknowledge that support. We would like to thank Professor T. G. Clapp, College of Textiles, North Carolina State University, for various useful discussions and suggestions. We would also like

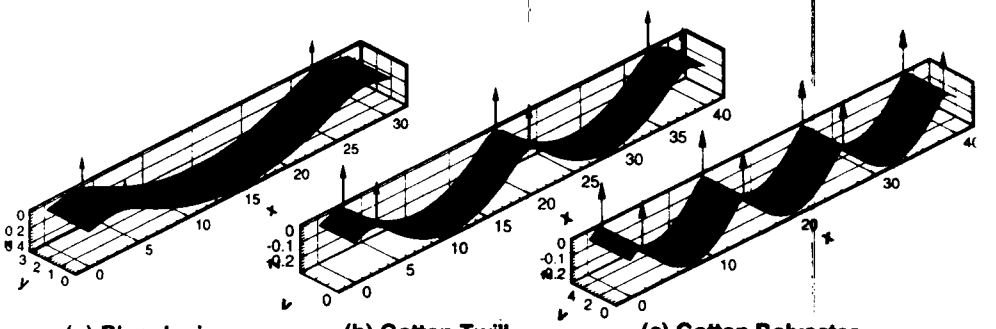

(a) Blue denim (b) Cotton Twill (c) Cotton Polyester

	l (cm)	b (cm)	α	x_1 (cm)	x_2 (cm)	x_3 (cm)	x_4 (cm)
(a)	30.5	3.0	221.4	3.62	26.88	-	-
(b)	40.0	3.0	1236.9	2.56	20.0	37.44	-
(c)	40.0	5.0	8744.7	1.54	13.87	26.13	38.46

FIGURE 7. Deformed shapes of fabric strips at optimal locations.

to acknowledge the excellent computing facilities of the North Carolina Supercomputing Center, which we used for the numerical results. We thank Medcovers Inc. for providing the dimensions of different products as well as the fabric samples.

Literature Cited

1. Cugini, U., Denti, P., and Rizzi, C., Design and Simulation of Non-rigid Materials Handling Systems, *Math. Comput. Simul.* **41**, 587–593 (1996).
2. Cugini, U., Denti, P., Ippolito, M., and Rizzi, C., Modeling and Simulation of Handling Machinery with Dynamic and Static Behavior of Non-rigid Materials, *IEEE Robot. Automat. Mag.* (3), 48–56 (1998).
3. Czarnecki, C., Automated Stripping: A Robotic Handling Cell for Garment Manufacture, *IEEE Robot. Automat. Mag.* (6), 4–8 (1995).
4. Deng, S., Nonlinear Fabric Mechanics Including Material Nonlinearity, Contact, and an Adaptive Global Solution Algorithm, Doctoral thesis, North Carolina State University, 1994.
5. Eischen, J. W., and Kim, Y. G., Optimization of Fabric Manipulation during Pick/Place Operations, *Int. J. Clothing Sci. Technol.* **5**(3/4), 68–76 (1993).
6. Eischen, J. W., Deng, S., and Clapp, T. G., Finite-Element Modeling and Control of Flexible Fabric Parts, *IEEE Comput. Graph. Appl.* (9), 71–80 (1996).
7. Fahantidis, N., Paraschidis, K., Petridis, V., Doulgeri, Z., Petrou, G., and Hasapis, G., Robot Handling of Flat Textile Materials, *IEEE Robot. Automat. Mag.* (3) 34–41 (1997).
8. Karakerezis, A., Ippolito, M., Doulgeri, Z., Rizz, C., Cugini, C., and Petridis, V., Robotic Handling of Flat Non-Rigid Materials, in "Proc. IEEE International Conference on Systems, Man and Cybernetics," 1994, pp. 937–946.
9. Kelley, C. T., "Iterative Methods for Optimization," No. 18 in Frontiers in Applied Mathematics, SIAM, Philadelphia, 1999.
10. Kolluru, R., Valavanis, K. P., Steward, A., and Sonnier, M. J., A Flat-Surface Robotic Gripper for Handling Limp Material, *IEEE Robot. Automat. Mag.* (9), 19–26 (1995).
11. Mroz, Z., and Rozvany, G. I. N., Optimal Design of Structures with Variable Support Conditions, *J. Optimiz. Theory Appl.* **15**(1), 85–101 (1975).
12. Narita, Y., Optimal Design of Support Location for Vibration of a Structure and its Components, *Curr. Topics Struct. Mech. ASME PVP* **179**, 169–173 (1989).
13. Olhoff, N., and Taylor, J. E., Designing Continuous Columns for Minimum Total Cost of Material and Interior Supports, *J. Struct. Mech.* **6**(4), 367–382 (1978).
14. Parker, J. K., Dubey, R., Paul, F. W., and Becker, R. J., Robotic Fabric Handling for Automating Garment Manufacturing, *ASME J. Eng. Ind.* 1–6 (1982).
15. Pitarresi, J. M., and Kunz, R. J., A Simple Technique for the Rapid Estimation of the Optimal Support Locations for a Vibrating Plate, *ASME J. Vibration Acoustics* **114**, 112–118 (1992).
16. Prager, W., and Rozvany, G. I. N., Plastic Design of Beams: Optimal Locations of Supports and Steps in Yield Moment, *Int. J. Mech. Sci.* **17**, 627–631 (1975).
17. Roschke, P. N., Optimal Pick-up Locations for Irregular

Concrete Panels, *Microcomput. Civil Eng.* **4,** 267–273 (1989).
18. Rozvany, G. I. N., and Mroz, Z., Column Design: Optimization of Support Conditions and Segmentation, *J. Struct. Mech.* **5**(3), 279–290 (1977).
19. Schweizerhof, K. H., and Wriggers, P., Consistent Linearization for Path Following Methods in Nonlinear FE Analysis, *Comput. Methods Appl. Mech. Eng.* **59,** 261–279 (1986).
20. Simo, J. C., and Fox, D. D., On a Stress Resultant Geometrically Exact Shell Model, Part I: Formulation and Optimal Parameterization, *Comput. Meth. Appl. Mech. Eng.* **72,** 267–304 (1989).
21. Simo, J. C., Fox, D. D., and Rifai, M. S., On a Stress Resultant Geometrically Exact Shell Model, Part II: The Linear Theory; Computational Aspects, *Comput. Meth. Appl. Mech. Eng.* **73,** 53–92 (1989).
22. Simo, J. C., Fox, D. D., and Rifai, M. S., On a Stress Resultant Geometrically Exact Shell Model, Part III: Aspects of the Nonlinear Theory, *Comput. Meth. Appl. Mech. Eng.* **79,** 21–70 (1990).
23. Taylor, P. M., Monkman, G. J., and Taylor, G. E., Electrostatic Grippers for Fabric Handling, in "Proc. IEEE International Conference on Robotics & Automation," 1988, pp. 431–433.
24. Torgerson, E., and Paul, F. W., Vision-Guided Robotic Fabric Manipulation for Apparel Manufacturing, *IEEE Control Sys. Mag.* (2), 14–20 (1988).
25. Wang, B. P., and Chen, C. L., Application of Genetic Algorithm for the Support Location Optimization of Beams, *Comput. Struct.* **58**(4), 797–800 (1996).
26. Wang, C. M., Xiang, Y., and Kitipornchai, S., Optimal Locations of Point Supports in Laminated Rectangular Plates for Maximum Fundamental Frequency, *Struct. Eng. Mech.* **5**(6), 691–703 (1997).
27. Xiang, Y., Wang, C. M., and Kitipornchai, S., Optimal Locations of Point Supports in Plates for Maximum Fundamental Frequency, *Struct. Optimiz.* **11,** 170–177 (1996).
28. Zhu, C., Byrd, R. H., Lu, P., and Nocedal, J., Algorithm 778: L-BFGS-B: Fortran Subroutines for Large-Scale Bound Constrained Optimization, *ACM Trans. Math. Software* **23**(4) 550–560 (1997).
29. The Fast System for the Objective Measurement of Fabric Properties: User's Manual. CSIRD, Australia.

Manuscript received September 23, 2002; accepted January 27, 2003.